White Matter Hyperintensities: Use of Aortic Arch Pulse Wave Velocity to Predict Volume Independent of Other Cardiovascular Risk Factors[1]

Kevin S. King, MD
Ke Xun Chen, BS
Keith M. Hulsey, PhD
Roderick W. McColl, PhD
Myron F. Weiner, MD
Paul A. Nakonezny, PhD
Ronald M. Peshock, MD

Purpose: To evaluate the relationship between pulse wave velocity (PWV) from the aortic arch and subsequent cerebral microvascular disease independent of other baseline cardiovascular risk factors among the participants in the multiethnic Dallas Heart Study.

Materials and Methods: Each subject gave written consent to participate in this HIPAA-compliant, institutional review board–approved prospective study. Aortic arch PWV was measured with phase-contrast magnetic resonance (MR) imaging in a population sample (n = 1270) drawn from the probability-based Dallas Heart Study. Seven years later, the volume of white matter hyperintensities (WMHs) was determined from brain MR images. Linear regression was conducted with aortic arch PWV, 15 other cardiovascular risk factors, and age, sex, and ethnicity included as predictors of WMH. The authors implemented a smoothly clipped absolute deviation–penalized variable selection method to evaluate an optimal predictive risk factor model.

Results: Aortic arch PWV helped predict WMH volume independent of the other demographic and cardiovascular risk factors (regression coefficient: 0.29; standard error: 0.06; 95% confidence interval: 0.17, 0.42; $P < .0001$). The optimal predictor variables of subsequent WMH volume adjusted for sex and ethnicity included aortic arch PWV, age, systolic blood pressure, hypertension treatment, and congestive heart failure. The authors estimated that a 1% increase in aortic arch PWV (in meters per second) is related to a 0.3% increase in subsequent WMH volume (in milliliters) when all other variables in the model are held constant.

Conclusion: Aortic arch PWV measured with phase-contrast MR imaging is a highly significant independent predictor of subsequent WMH volume, with a higher standardized effect than any other cardiovascular risk factor assessed except for age. In an optimal predictive model of subsequent WMH burden, aortic arch PWV provides a distinct contribution along with systolic blood pressure, hypertension treatment, congestive heart failure, and age.

Supplemental material: *http://radiology.rsna.org/lookup/suppl/doi:10.1148/radiol.13121598/-/DC1*

[1] From the Department of Radiology (K.S.K., K.X.C., K.M.H., R.W.M., R.M.P.), Departments of Psychiatry and Neurology (M.F.W.), Department of Clinical Sciences, Division of Biostatistics (P.A.N.), Department of Internal Medicine (R.M.P.), and Reynolds Cardiovascular Clinical Research Center (R.M.P.), University of Texas Southwestern Medical Center, 5323 Harry Hines Blvd, Dallas, TX 75390. Received August 15, 2012; revision requested October 1; revision received November 5; accepted November 14; final version accepted December 5. Supported by a center grant from the Donald W. Reynolds Foundation. **Address correspondence to** K.S.K. (e-mail: *kevin.king@utsouthwestern.edu*).

This publication was supported by grant no. KL2RR024983, titled "North and Central Texas Clinical and Translational Science Initiative" (Robert Toto, MD, principle investigator), from the National Center for Research Resources (NCRR), a component of the National Institutes of Health (NIH), and NIH Roadmap for Medical Research, and its contents are solely the responsibility of the authors and do not necessarily represent the official views of the NCRR or NIH. The Dallas Heart Study was also supported by a center grant from the Donald W. Reynolds Foundation. This work was conducted with support from UT Southwestern Clinical and Translational Alliance for Research (UT-STAR, NIH/National Center for Advancing Translational Sciences grant nos. UL1RR024982 and TR00045106. The content is solely the responsibility of the authors and does not necessarily represent the official views of UT-STAR, the University of Texas Southwestern Medical Center at Dallas and its affiliated academic and health care centers, the National Center for Advancing Translational Sciences, or the NIH.

White matter hyperintensities (WMHs), which are presumably sequela of microvascular ischemic disease (1), are associated with accelerated motor and cognitive decline, stroke, and death (2). Cerebral microvascular disease may often coexist with illnesses or conditions that lead to dementia, lowering the threshold for disease expression (1). To formulate treatment and prevention strategies, it is essential to understand the mechanisms underlying cerebral microvasculature disease. Hypertension has repeatedly been identified as a primary risk factor (3,4). The high resting blood flow and low vascular resistance in the cerebral circulation may make it particularly susceptible to damage from pulsatile blood flow (5).

Aortic stiffness, a key determinant of pulsatile flow as well as an indicator of target organ damage (6), has been shown to improve prediction of diverse cardiovascular events and all-cause mortality (7). More recent work has demonstrated an association between aortic stiffness and cerebrovascular disease (8–12).

The aortic arch, from which the cerebral circulation arises, has a different compliance at baseline and experiences different rates of change in compliance with aging compared with the remainder of the aorta (13). In addition, it may have a distinct association with cerebral microvascular disease (9). In the healthy state, there is a difference in compliance between the highly elastic aorta and the more muscular branch vessels, including the carotid and renal arteries (9,14). This vascular impedance mismatch results in partial reflection of the pulse wave, potentially protecting the microvasculature. With aging there is greater loss of compliance in the aorta than in the branch vessels, resulting in impedance matching (14) and diminished wave reflection (9,15). Phase-contrast magnetic resonance (MR) imaging may therefore have utility for studying the importance of compliance on the development of chronic cerebrovascular disease by accurately measuring pulse wave velocity (PWV) (16) from only the aortic arch, where the cerebral circulation arises. Previous physiology studies evaluating the association between PWV from the entire aorta and WMH have mixed results, with some studies showing a highly significant independent association (8,9) and others showing that the association is attenuated (10) or loses significance with adjustment for blood pressure and standard cardiovascular risk factors (11,12).

To our knowledge, no large population-based study has evaluated the PWV from the aortic arch with phase-contrast MR imaging and its importance in enabling the prediction of WMH volume at a later point in time. The purpose of our study was to evaluate the association between PWV from the aortic arch and subsequent cerebral microvascular disease independent of other baseline cardiovascular risk factors among the participants in the multiethnic Dallas Heart Study (DHS).

Advances in Knowledge

- Aortic arch pulse wave velocity (PWV) is an independent predictor ($P < .0001$) of subsequent white matter hyperintensity (WMH) volume, with a greater standardized effect and level of significance than all other cardiovascular risk factors assessed except for age.
- In an optimal predictive model, aortic arch PWV provides a distinct contribution to WMH burden along with systolic blood pressure, hypertension treatment, history of congestive heart failure, and age.

Materials and Methods

Study Population and Participants

The subject sample was drawn from the DHS, a large population-based, multiethnic, multistep, probability-based study of civilian noninstitutionalized English- or Spanish-speaking Dallas County residents with oversampling of African Americans. The DHS was designed to produce unbiased population estimates of biologic and social variables, as previously described (17). Each participant gave written consent to participate in this Health Insurance Portability and Accountability Act–compliant, institutional review board–approved prospective study. There were two waves to the study, DHS-1 and DHS-2, and they were performed approximately 7 years apart.

In DHS-1, 2596 participants underwent aorta and cardiac imaging and clinical evaluation. Of those 2596 subjects, 1320 returned for DHS-2 and completed brain imaging. These subjects were eligible for inclusion in our study. Of those 1320 subjects, 33 were excluded because of self-reported history of stroke and 17 because an image artifact or observed abnormality precluded automated analysis. Thus, 1270 subjects participated in our study.

Implication for Patient Care

- PWV from the aortic arch provides functional information about vessel compliance that may help determine risk for cerebrovascular disease.

Published online before print
10.1148/radiol.13121598 **Content code:** CA

Radiology 2013; 267:709–717

Abbreviations:
DHS = Dallas Heart Study
FOV = field of view
OLS = ordinary least squares
PWV = pulse wave velocity
SCAD = smoothly clipped absolute deviation
WMH = white matter hyperintensity

Author contributions:
Guarantors of integrity of entire study, K.S.K., R.M.P.; study concepts/study design or data acquisition or data analysis/interpretation, all authors; manuscript drafting or manuscript revision for important intellectual content, all authors; manuscript final version approval, all authors; literature research, K.S.K., K.X.C., R.M.P.; clinical studies, K.S.K., R.M.P.; statistical analysis, K.S.K., K.X.C., R.W.M., P.A.N.; and manuscript editing, K.S.K., K.X.C., R.W.M., M.F.W., P.A.N., R.M.P.

Funding:
This research was supported by the National Institutes of Health (grants KL2RR024983, UL1RR024982, and TR00045106).

Conflicts of interest are listed at the end of this article.

Outcome Variable

The outcome measure for our study was WMH volume (in milliliters) automatically quantified from two-dimensional fluid-attenuated inversion recovery and three-dimensional magnetization-prepared rapid acquisition gradient-echo brain images obtained during follow-up evaluation as part of DHS-2 with a 3.0-T MR unit (Achieva; Philips Medical Systems, Best, the Netherlands). Our WMH segmentation method and validation has previously been described (18). In brief, initial tissue segmentation was based on a processing algorithm of magnetization-prepared rapid acquisition gradient-echo imaging by using the freely available FSL software (FMRIB Software Library, available at *http://fsl.fmrib.ox.ac.uk/fsl/fslwiki/*) and three FSL command-line tools: BET (brain extraction and/or extrameningeal tissue removal) (19), FAST (intensity-based segmentation to generate gray and/or white and/or cerebrospinal fluid and the gray and/or white periphery) (20), and FIRST (model-based segmentation to extract subcortical gray matter and identify the brainstem and cerebellum) (21). The white matter masks generated were transformed to fluid-attenuated inversion recovery images by using the FLIRT tool of the FSL software (22). WMHs were automatically identified from the white matter mask by using a threshold of 3 standard deviations above the mean fluid-attenuated inversion recovery signal intensity from the cerebral periphery to limit skewing of the signal intensity distribution from hyperintense periventricular white matter voxels. The brainstem and cerebellum were excluded from this analysis. Parameters for two-dimensional fluid-attenuated inversion recovery imaging were as follows: 32 sections were acquired with 11 000/130/2800 (repetition time msec/echo time msec/inversion time msec), echo train length of 44, sensitivity encoding factor of 2, field of view (FOV) of 250 × 250 mm, 4-mm-thick sections with a 1-mm gap between sections, and matrix of 240 × 138, yielding a voxel size of 4 × 0.96 × 1.33 mm = 5.11 mm^3. Three-dimensional magnetization-prepared rapid acquisition gradient-echo imaging was performed with the following parameters: axial sections reconstructed at 1.0-mm section thickness, 9.6/5.8 (repetition time msec/echo time msec), 12° flip angle, and 260 × 260-mm FOV.

Predictor Variables

The primary predictor variable in the current study was PWV from the aortic arch. Images were acquired as part of DHS-1 by using two comparable 1.5-T MR units (ACS-NT and Intera, Philips Medical Systems). A cardiac-gated, through-plane flow sequence (velocity-encoding value, 150 cm/sec through plane; FOV, 34 cm; 10/5; temporal resolution, 40 msec) was performed in the transverse plane at the level of the pulmonary artery to image the ascending and descending aorta in cross section. The time-velocity curve was interpolated to a temporal resolution of 10 msec by using a cubic spine for subsequent analysis. A second, oblique, double inversion-recovery spin-echo image (FOV, 33 cm; electrocardiographically gated repetition time; echo time, 5.3 msec; echo train length, 32) was obtained through the ascending aorta, transverse portion of the aortic arch, and descending aorta (termed the "candy cane" view). A scout line indicating the position of the phase-contrast acquisition image plane was displayed on the candy cane view of the aortic arch. With use of ImageJ software (National Institutes of Health, Bethesda, Md), the aortic arch distance was determined by drawing a freehand line through the center of the aorta parallel to the aortic walls between the positions in the ascending and descending aorta at which the arterial flow was measured, as indicated by the scout line. This distance was termed the aortic arch distance. PWV was calculated by dividing the aortic arch distance by the transit time, which was calculated as the time between the ascending and descending upstroke velocities at half maximum (23–25). Further details regarding aortic arch PWV measurement are shown in the Figure.

Cardiovascular risk factors.—Variables were assessed at entry into DHS-1. Continuous measurements included systolic and diastolic blood pressure (in millimeters of mercury) measured five times with an automated oscillometric device (Welch Allyn, Skaneateles Falls, NY), with the reported value taken from the average of the third to fifth recordings, heart rate (in beats per minute), and body mass index. The following risk factors were binary indicator variables operationalized as the presence or absence of the condition (with "absence of the condition" being the reference group): abnormal glucose tolerance (fasting glucose level of ≥100 mg/dL or nonfasting glucose level of ≥140 mg/dL or treatment), elevated serum triglyceride level (fasting triglyceride level of ≥150 mg/dL or treatment), low serum high-density lipoprotein level (<40 mg/dL for men and <50 mg/dL for women or treatment), and large waist circumference (>102 cm for men and >88 cm for women). These values were calculated according to National Institutes of Health Cholesterol Education Program ATP III Guidelines (26). Hypercholesterolemia was defined as calculated low-density lipoprotein cholesterol level greater than 160 mg/dL (4.1 mmol/L) with a fasting sample, direct low-density lipoprotein cholesterol level greater than 160 mg/dL (4.1 mmol/L) with a nonfasting sample, total cholesterol level greater than 200 mg/dL (5.2 mmol/L), or use of statin medication. Diabetes mellitus was defined either through self-report accompanied by use of antihyperglycemic medication or as an elevated serum glucose level (fasting glucose level >126 mg/dL [7.0 mmol/L], nonfasting glucose level >200 mg/dL [11.1 mmol/L]). History of smoking was classified as "never smoked" or "current or former smoker." Hypertension treatment and diagnosis by a health care professional of congestive heart failure or myocardial infarction were self-reported.

The cardiac MR imaging protocol for the DHS consisted of short-axis breath-hold electrocardiographically gated cine MR imaging from the apex to the base of the left ventricle with use of the following parameters: 6-mm-thick sections, 4-mm gap, 36–40-cm FOV, acquired pixel size at 36-cm FOV of 1.29

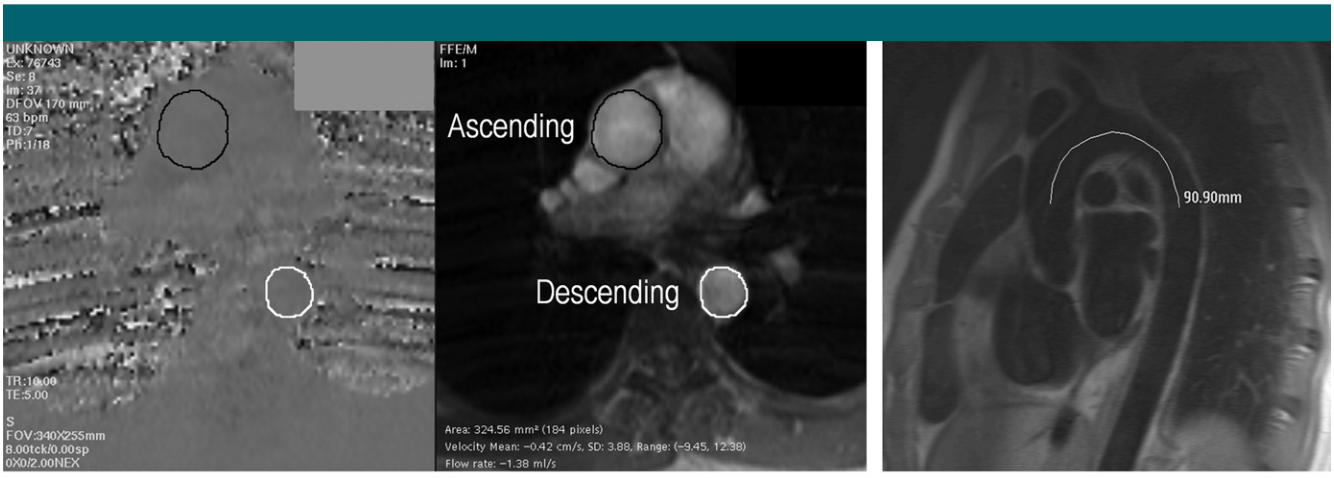

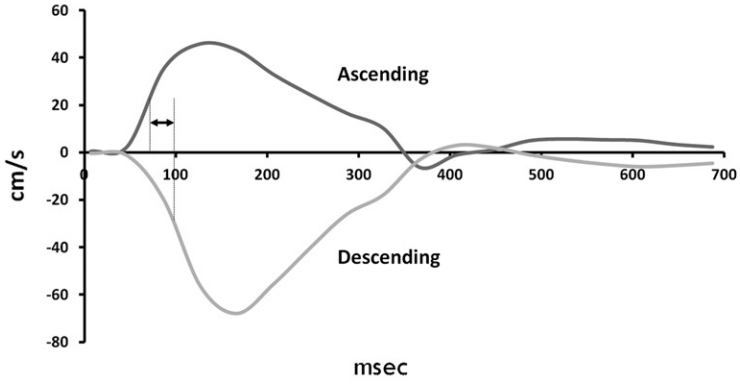

Measurement of PWV at phase-contrast MR imaging. **(a)** Phase-contrast (left) and magnitude (right) MR images obtained with cardiac-gated flow sequence demonstrate method for measuring flow velocity in ascending (black circles) and descending (white circles) aorta. **(b)** Graph shows time points of half maximum velocity in ascending (dark gray line) and descending (light gray line) aorta, which are used to determine time elapsed (arrow) as pulse wave traverses aortic arch. **(c)** Double inversion-recovery spin-echo candy cane view of aorta shows distance traversed. PWV is calculated by dividing distance by time.

× 2.58, and temporal resolution of 40 msec. Software (MASS; Medis Medical Imaging Systems, Leiden, the Netherlands) was used to analyze the data. Endocardial and epicardial borders were traced manually, allowing calculation of left ventricular wall volumes. Left ventricular hypertrophy was derived from the left ventricular mass normalized to derived body surface area by using a previously described method (27).

Demographic factors.—The demographic variables were age at the time of MR imaging (in years), sex (with male as the reference group), and race (African American and Hispanic subjects compared with white subjects as the reference group).

Statistical Analysis

Demographic and clinical characteristics for the overall sample were described by using the sample mean and standard deviation for continuous variables and the frequency and percentage for categorical variables. WMH volume and aortic PWV were log-transformed to obtain a more normal distribution. Multiple linear regression with ordinary least squares (OLS) estimation was conducted on the log of WMH volume from DHS-2 (as the outcome variable), with the log of aortic PWV and the 15 cardiovascular risk factors assessed at DHS-1 and four demographic variables included in the model as predictors (covariates). We also implemented the smoothly clipped absolute deviation (SCAD)–penalized variable selection method (28), in the context of a linear regression model, with the log of WMH volume as the outcome variable and with sex and race "forced in" the final model. The goal of the SCAD-penalized regression is to select a parsimonious and well-fitting subset of potential predictor variables for a linear regression and automatically fit an adjusted regression equation to this subset. SCAD-penalized regression, as described by Fan and Li (28), is a way of constructing a regression model by doing predictor variable selection and coefficient estimation together. This is done by optimizing a penalized least squares criterion that expresses a balance between good fit and parsimony. One such penalty function is the SCAD penalty (28). Given the size of our sample (n = 1270), we chose a more "heavily penalized" SCAD model, which is based on the Bayesian information criterion and is less likely to include unimportant variables. For an in-depth explication of the theory and technical details of SCAD-penalized estimation, we refer the reader to the work of Fan and Li (28).

We performed all statistical analyses by using software (SAS, version 9.2; SAS Institute, Cary, NC). The

Table 2

Optimal Predictive Model for WMH Volume with a SCAD-penalized Variable Selection Method

Variable	SCAD Parameter Estimate*	OLS Parameter Estimate†	OLS *P* Value‡	OLS Standardized Estimate§	OLS Variance Inflation Factor
Female	0.124 ± 0.041	0.127 ± 0.041	.002	0.078	1.040
African American	0.035 ± 0.045	0.019 ± 0.046	.679	0.012	1.289
Hispanic	0.127 ± 0.062	0.113 ± 0.062	.070	0.049	1.185
Age	0.026 ± 0.003	0.025 ± 0.003	<.0001	0.285	1.674
Log of aortic arch PWV	0.336 ± 0.063	0.309 ± 0.063	<.0001	0.154	1.634
Systolic blood pressure	0.003 ± 0.001	0.004 ± 0.001	.003	0.085	1.295
Hypertension treatment	0.049 ± 0.024	0.124 ± 0.063	.050	0.054	1.220
Congestive heart failure	0.417 ± 0.141	0.520 ± 0.164	.002	0.080	1.038

Note.—Data are for 1270 subjects. A 1% increase in aortic arch PWV (in meters per second) is related to a 0.335% increase $\{[(1.01)^{0.336} - 1] \times 100\}$ for the SCAD-penalized regression model and a 0.308% increase $\{[(1.01)^{0.309} - 1] \times 100\}$ for the OLS regression model in subsequent WMH volume (in milliliters), respectively, when all other variables in the models are held constant. Final model $R^2 = 0.224$, adjusted $R^2 = 0.219$.

* Data are SCAD-penalized least squares regression coefficients ± robust sandwich standard error estimates.

† Data are OLS unstandardized regression coefficients ± standard error estimates.

‡ OLS linear regression *P* values, which are two sided, are associated with the OLS parameter estimates and standard errors.

§ Data are standardized regression coefficients from OLS regression.

level of significance for all tests was set at $\alpha = 0.05$ (two-tailed). The procedures of PROC REG in SAS software were used to conduct the OLS multiple linear regression analysis. The procedures of PROC SCADLS (version 1.1.1; The Methodology Center, Penn State, University Park, Pa, available at *http://methodology.psu.edu*) were used to implement the SCAD-penalized variable selection method in the context of a linear regression model.

To ascertain the presence of any multicollinearity in our linear regression models, we examined the variance inflation factor for each of the predictors in each model. The estimated variance inflation factors for the predictors were all close to 1 and less than 5 (Tables 1, 2), which suggests that multicollinearity was not present or problematic for any of the covariates in our linear regression models.

Results

Participant Characteristics

The mean age of our sample (1270 DHS participants meeting study inclusion and exclusion criteria as discussed earlier) at the time of brain imaging in DHS-2 was 51.4 years ± 9.4 (standard deviation). The mean age of the 708

Table 1

Predictors of Log of WMH Volume at Multiple Linear Regression Analysis

Variable	Parameter Estimate*	*P* Value†	Standardized Estimate‡	VIF§
Female	0.147 ± 0.044	.001	0.090	1.188
African American	0.016 ± 0.048	.743	0.010	1.404
Hispanic	0.135 ± 0.063	.034	0.058	1.217
Age	0.024 ± 0.003	<.0001	0.278	1.829
Log of aortic PWV	0.298 ± 0.064	<.0001	0.149	1.673
Left ventricular hypertrophy	−0.070 ± 0.081	.388	−0.024	1.199
Systolic blood pressure	0.005 ± 0.002	.059	0.098	4.348
Diastolic blood pressure	−0.001 ± 0.004	.782	−0.013	3.679
Heart rate	0.002 ± 0.002	.408	0.022	1.153
Hypertension treatment	0.139 ± 0.064	.031	0.061	1.278
Congestive heart failure	0.528 ± 0.168	.002	0.082	1.098
Myocardial infarction	−0.061 ± 0.176	.730	−0.009	1.083
History of smoking	0.037 ± 0.042	.380	0.022	1.051
Abnormal glucose tolerance	0.019 ± 0.056	.735	0.010	1.434
Elevated triglycerides	0.029 ± 0.052	.580	0.015	1.238
Low HDL level‖	−0.041 ± 0.045	.360	−0.025	1.173
High total cholesterol	0.070 ± 0.065	.284	0.028	1.082
Large waist circumference	−0.023 ± 0.056	.679	−0.014	1.975
Diabetes	0.008 ± 0.092	.930	0.003	1.348
Body mass index	−0.007 ± 0.005	.166	−0.048	1.934

Note.—Data are from 1262 subjects because body mass index was missing for eight subjects. A 1% increase in aortic arch PWV (in meters per second) is related to a 0.297% increase $\{[(1.01)^{0.298} - 1] \times 100\}$ in subsequent WMH volume (in milliliters) when all other variables in the model are held constant. Model $R^2 = 0.232$, adjusted $R^2 = 0.219$.

* Data are unstandardized regression coefficients ± standard errors.

† *P* values are two sided.

‡ Data are standardized regression coefficients.

§ VIF = variance inflation factor.

‖ HDL = high-density lipoprotein.

Table 3

Summary of Demographic and Clinical Characteristics

Parameter	Value
Mean age (y)	51.4 ± 9.4
No. of women	708 (55.7)
Race	
African American	553 (43.5)
White	506 (39.8)
Hispanic	183 (14.4)
Other	28 (2.2)
Mean WMH volume (mL)	1.6 ± 3.6
Mean aortic arch PWV (m/sec)	4.8 ± 2.8
Mean blood pressure (mm Hg)	
Systolic	125.4 ± 17.2
Diastolic	78.5 ± 9.7
Mean heart rate (beats/min)	74.6 ± 11.0
Mean body mass index (kg/m^2)	28.2 ± 5.8
Diabetes	89 (7.0)
Elevated triglyceride level	303 (23.8)
Abnormal glucose tolerance	314 (24.7)
Low HDL level*	489 (38.5)
High total cholesterol level	146 (11.5)
Large waist circumference	607 (47.8)
Current or prior smoker	523 (41.2)
Hypertension treatment	184 (14.5)
Congestive heart failure	20 (1.6)
Myocardial infarction	18 (1.4)
Left ventricular hypertrophy	102 (8.0)

Note.—Except where indicated, data are numbers of subjects (n = 1270), with percentages in parentheses. WMH volume and patient age were assessed at DHS-2. The remaining characteristics were assessed at DHS-1.

* HDL = high-density lipoprotein.

female participants, who comprised 56% of our sample, was 51.6 years ± 9.6. The mean age of the 562 male participants was 51.2 years ± 9.1. There was no significant age difference between sexes (P = .54, t test). The ethnic distribution was as follows: 553 of the 1270 subjects (43.5%) were African American, 506 (39.8%) were white, and 183 (14.4%) were Hispanic. Twenty-eight subjects (2.2%) were of another race. One hundred two subjects (8%) had left ventricular hypertrophy at MR imaging. One hundred eighty-four of the 1270 subjects (14.5%) self-reported a history of hypertension treatment, and 20 (1.6%) reported a history of congestive heart failure. The average systolic and diastolic blood pressure was 125.4 mm Hg ± 17.2 and 78.5 mm Hg ± 9.8, respectively. The average body mass index was 28.2 kg/m^2 ± 5.8. The average WMH volume was 1.6 mL ± 3.6, with a median of 0.88 mL (interquartile range, 0.58–1.41 mL). The average aortic arch PWV was 4.8 m/sec ± 2.8, with a median of 4.2 m/sec (interquartile range, 3.3–5.5 m/sec). Participant characteristics are summarized in Table 3.

The initial DHS-1 group of 2596 subjects with complete aortic arch PWV and cardiac MR imaging and initial clinical evaluation had a slightly lower proportion of female subjects (n = 1418, 54.6%) and a higher proportion of Hispanics (n = 450, 17.3%) and African Americans (n = 1264, 48.7%) compared with our final sample. For the main predictors in our final model, the initial DHS-1 group had slightly higher mean aortic PWV (5.0 m/sec ± 3.1) and systolic blood pressure (127.8 mm Hg ± 19.3) as well as a higher proportions of subjects undergoing hypertension treatment (n = 470, 18.1%) and with a history of congestive heart failure (n = 82, 3.2%). Our final study sample was therefore composed of individuals from DHS-1 with slightly lower risk factor severity, which may lower the observable effect from the predictors in our model.

WMH and Aortic Arch PWV

Results of OLS multiple linear regression revealed that aortic arch PWV at study entry was a significant predictor of subsequent WMH volume 7 years later when adjusting for all the other demographic and cardiovascular risk factors (unstandardized regression coefficient = 0.29; standard error = 0.06; 95% confidence interval: 0.17, 0.42; $P < .0001$). The OLS regression analysis also revealed that, among the cardiovascular risk factors in the model other than age, aortic arch PWV had the greater statistical significance and magnitude of effect in the expected relationship with subsequent WMH volume (as interpreted from the standardized regression coefficient estimate of 0.148). The OLS regression results from the full model suggest that aortic arch PWV had a significant positive linear relationship with subsequent WMH volume while adjusting for the other demographic and cardiovascular risk factors. However, to interpret the positive linear relationship between aortic arch PWV and subsequent WMH volume—because both WMH and aortic arch PWV were log-transformed to a natural log scale—we back-transformed the unstandardized parameter estimate (0.298) into the original metric. Thus, for the full OLS regression model (where the unstandardized parameter estimate is 0.298; Table 1), in which the appropriate back transformation was applied when both the outcome and predictor are log-transformed, we estimate that a 1% increase in aortic arch PWV is related to a 0.297% increase $\{[(1.01)^{0.298} - 1] \times 100\}$ in subsequent WMH volume when all other variables in the model are held constant. In other words, when all other variables in the model are held constant, we estimate about a 0.29% increase in subsequent WMH volume when aortic arch PWV increases by 1%. The OLS regression results for the full model, with all predictor variables included, are shown in Table 1. (For expanded tables with more comprehensive statistical details, please see Tables E1 and E2 [online].)

The subset of predictor variables that were selected from the SCAD-penalized variable selection method are reported in Table 2. With sex and race "forced in" the final model, the SCAD-penalized least squares linear regression revealed that aortic arch PWV, age, systolic blood pressure, hypertension treatment, and congestive heart failure were significant predictors of subsequent WMH volume at year 7. As shown in Table 2, for the subset of retained predictor variables both the SCAD-penalized and OLS parameter estimates (and standard errors) were of similar magnitude and suggested that aortic arch PWV had a significant positive linear relationship with subsequent WMH volume (where the unstandardized parameter estimates were 0.336 and 0.309 for the SCAD-penalized and OLS regression models, respectively). Thus, for both the SCAD-penalized and

OLS regression coefficients (from Table 2)—with application of the aforementioned back transformation—we estimate that a 1% increase in aortic arch PWV is related to a 0.335% increase $\{[(1.01)^{0.336} - 1] \times 100\}$ and a 0.308% increase $\{[(1.01)^{0.309} - 1] \times 100\}$, respectively, in subsequent WMH volume when all other variables in the models are held constant.

Discussion

Our findings indicate that aortic arch PWV, as derived with phase-contrast MR imaging, helps predict subsequent WMH volume ($P < .0001$) independent of a broad range of demographic and cardiovascular risk factors in a multiethnic population–based sample ($n = 1270$). This included adjusting for systolic and diastolic blood pressure, which addresses potential effects of aortic stiffening on blood pressures at one point in time as well as left ventricular hypertrophy, which is generally a reflection of hypertensive effects over a period of time. Despite adjusting for numerous covariates, there was no evidence of significant multicollinearity for aortic arch PWV. These results provide evidence of a link between large-vessel disease in the aortic arch and small-vessel disease in the brain.

We then evaluated the relative contribution of aortic arch PWV in an optimal predictive model of subsequent WMH volume derived with a SCAD-penalized variable selection method (optimizing a penalized least squares criterion that expresses a balance between good fit and parsimony) while adjusting for sex and race. With use of this method, the optimal model consisted of age, aortic arch PWV, systolic blood pressure, hypertension treatment, and history of congestive heart failure, with each providing independent contributions to the prediction of WMH volume. Aortic arch PWV emerged as the primary predictor of WMH apart from age, with a greater statistical significance and standardized coefficient of effect than any of the other factors in either the full model or the optimal predictive model.

Stiffening of the aortic arch may alter transmission of pulsatile hemodynamic forces to the anterior circulation of the brain distinct from its influence on systemic blood pressures (9). The healthy aortic arch has a higher compliance than the brachiocephalic and common carotid arteries. The relationship of higher compliance to slower wave velocity is described in models as impedance. When pressure waves encounter a site of impedance mismatch, a portion of the wave is reflected. With aging, there is a more rapid decrease in compliance of the aorta than its branch vessels and the protective effects of impedance mismatch may be lost (9,13).

The results of our study are best understood in the context of the growing evidence supporting aortic stiffness as a significant independent predictor of cardiovascular disease, including all-cause mortality (7) and fatal stroke (29). Aortic PWV is a forceful marker that improves determination of risk for cardiovascular events both in indicating higher risk among those with otherwise low risk as well as further stratification among those already identified as at risk (30–32). In particular, our results are in keeping with those from previous large studies evaluating associations between carotid femoral aortic PWV measured by means of applanation tonometry and WMH volume (8,9,33). The method used for WMH assessment may explain some of the discrepancy in previous aortic PWV studies, as studies with continuous volumetric assessment of WMH demonstrated a persistent association (8,9,33) whereas those losing significance used a visual scale (11,12).

A previous study using phase-contrast MR imaging to determine PWV from the aortic arch in a modestly sized ($n = 50$) sample of patients with hypertension showed an association with concurrently measured WMH burden, which became insignificant after adjusting for age, sex, and hypertension duration (34). Data from our population-based study ($n = 1270$), however, demonstrated PWV from the aortic arch obtained with phase-contrast MR imaging to be a highly significant independent predictor of subsequent WMH volume ($P < .0001$). It can be speculated that the previous study may have suffered from insufficient power owing to lower numbers of participants. This is supported by a follow-up study by this same group of a slightly larger size ($n = 86$) performed in patients with type 1 diabetes mellitus, which demonstrated an independent association between aortic PWV and WMH after adjustment for other risk factors (35).

A limitation of our study is the lack of baseline brain MR imaging at study entry during DHS-1. Aortic arch PWV measurements were obtained from 7 years before brain MR imaging. As a group, we can be certain that WMH burden will increase during this time. Still, it is not possible to delineate what component of WMH is incident since the time of aortic arch PWV measurement at study entry. Furthermore, although the association between aortic arch PWV and WMH persisted after adjustment for numerous cardiovascular risk factors, their association may still reflect related end-organ disease. Future work to elucidate the underlying pathophysiology will need to assess the complex interaction between cardiac physiology and aortic stiffness (36). Herein, we account for two of the more significant hemodynamic associations of aortic stiffness: blood pressure and left ventricular hypertrophy (6,37–39). Future studies would benefit from evaluating directly the interaction of cardiac physiology with aortic stiffness.

A second limitation of our study is the use of relatively low temporal resolution imaging of 40 msec for the velocity-encoded MR imaging sequence used to derive the aortic arch PWV. This reflects in part the limitations in acquiring this sequence as part of a population-based trial with limited imaging time for each sequence and use of the 1.5-T technology available to us at that time. This loss of granularity was thought unlikely to unduly limit significant associations in our population-based trial but does limit the precision of data from any given individual. This would be expected to have the effect of introducing additional noise to our aortic arch PWV measurement that would tend to lessen the degree of

association. This creates an increased likelihood of failing to detect a significant difference when one truly exists but would not be expected to contribute to the strong association seen for aortic arch PWV in our study. Another potential criticism of our technique is that the foot of the wave is more conventionally used to estimate wave arrival time because this time point only reflects wave propagation and is not influenced by central augmentation or distal dampening of the pulse. Given the close relationship between the points of measurement, both of which were obtained centrally from the aortic arch, this is less likely to be significant compared with tonometry measurements from distal components of the arterial tree. With our curve-fitting technique we found that half maximum velocity was more accurate than the foot of the slope owing to errors in extrapolating the intersection of baseline and upstroke velocities. There is precedent for using the point of half maximum to estimate arrival time at MR imaging (23,24), and this methodology has been shown in a recent study to have higher correlation with age and carotid femoral PWV (25).

Further studies are needed to affirm prognostic and therapeutic implications of our findings. PWV from the aortic arch provides functional information about vessel compliance that may help determine the risk for cerebrovascular disease. PWV from localized aortic segments may also be useful in determining which individuals might benefit from selective hypertension medication (40,41) to decrease propagation of pulsatile energy to specific vascular beds (5).

In conclusion, PWV from the aortic arch is an independent predictor of subsequent WMH volume and emerges as the primary cardiovascular risk factor of WMH after age. In an optimal predictive model, PWV from the aortic arch provides a distinct contribution to WMH burden along with systolic blood pressure, hypertension treatment, history of congestive heart failure, and age.

Acknowledgment: We thank Akshay Goel for assistance with manuscript revision.

Disclosures of Conflicts of Interest: K.S.K. No relevant conflicts of interest to disclose. **K.X.C.** No relevant conflicts of interest to disclose. **K.M.H.** No relevant conflicts of interest to disclose. **R.W.M.** No relevant conflicts of interest to disclose. **M.F.W.** No relevant conflicts of interest to disclose. **P.A.N.** No relevant conflicts of interest to disclose. **R.M.P.** Financial activities related to the present article: none to disclose. Financial activities not related to the present article: received travel and hotel meeting expenses from Philips Medical Systems. Other relationships: none to disclose.

References

1. Black S, Gao F, Bilbao J. Understanding white matter disease: imaging-pathological correlations in vascular cognitive impairment. Stroke 2009;40(3 Suppl):S48–S52.
2. Debette S, Markus HS. The clinical importance of white matter hyperintensities on brain magnetic resonance imaging: systematic review and meta-analysis. BMJ 2010;341:c3666.
3. Longstreth WT Jr, Manolio TA, Arnold A, et al. Clinical correlates of white matter findings on cranial magnetic resonance imaging of 3301 elderly people: the Cardiovascular Health Study. Stroke 1996;27(8):1274–1282.
4. Basile AM, Pantoni L, Pracucci G, et al. Age, hypertension, and lacunar stroke are the major determinants of the severity of age-related white matter changes: the LADIS (Leukoaraiosis and Disability in the Elderly) study. Cerebrovasc Dis 2006;21(5-6):315–322.
5. O'Rourke MF, Safar ME. Relationship between aortic stiffening and microvascular disease in brain and kidney: cause and logic of therapy. Hypertension 2005;46(1):200–204.
6. Laurent S, Cockcroft J, Van Bortel L, et al. Expert consensus document on arterial stiffness: methodological issues and clinical applications. Eur Heart J 2006;27(21):2588–2605.
7. Vlachopoulos C, Aznaouridis K, Stefanadis C. Prediction of cardiovascular events and all-cause mortality with arterial stiffness: a systematic review and meta-analysis. J Am Coll Cardiol 2010;55(13):1318–1327.
8. Coutinho T, Turner ST, Kullo IJ. Aortic pulse wave velocity is associated with measures of subclinical target organ damage. JACC Cardiovasc Imaging 2011;4(7):754–761.
9. Mitchell GF, van Buchem MA, Sigurdsson S, et al. Arterial stiffness, pressure and flow pulsatility and brain structure and function: the Age, Gene/Environment Susceptibility–Reykjavik Study. Brain 2011;134(Pt 11):3398–3407.
10. Henskens LH, Kroon AA, van Oostenbrugge RJ, et al. Increased aortic pulse wave velocity is associated with silent cerebral small-vessel disease in hypertensive patients. Hypertension 2008;52(6):1120–1126.
11. Kim DH, Kim J, Kim JM, Lee AY. Increased brachial-ankle pulse wave velocity is independently associated with risk of cerebral ischemic small vessel disease in elderly hypertensive patients. Clin Neurol Neurosurg 2008;110(6):599–604.
12. Hatanaka R, Obara T, Watabe D, et al. Association of arterial stiffness with silent cerebrovascular lesions: the Ohasama study. Cerebrovasc Dis 2011;31(4):329–337.
13. Rogers WJ, Hu YL, Coast D, et al. Age-associated changes in regional aortic pulse wave velocity. J Am Coll Cardiol 2001;38(4):1123–1129.
14. Hashimoto J, Ito S. Some mechanical aspects of arterial aging: physiological overview based on pulse wave analysis. Ther Adv Cardiovasc Dis 2009;3(5):367–378.
15. Webb AJ, Simoni M, Mazzucco S, Kuker W, Schulz U, Rothwell PM. Increased cerebral arterial pulsatility in patients with leukoaraiosis: arterial stiffness enhances transmission of aortic pulsatility. Stroke 2012;43(10):2631–2636.
16. Grotenhuis HB, Westenberg JJ, Steendijk P, et al. Validation and reproducibility of aortic pulse wave velocity as assessed with velocity-encoded MRI. J Magn Reson Imaging 2009;30(3):521–526.
17. Victor RG, Haley RW, Willett DL, et al. The Dallas Heart Study: a population-based probability sample for the multidisciplinary study of ethnic differences in cardiovascular health. Am J Cardiol 2004;93(12):1473–1480.
18. Hulsey KM, Gupta M, King KS, Peshock RM, Whittemore AR, McColl RW. Automated quantification of white matter disease extent at 3 T: comparison with volumetric readings. J Magn Reson Imaging 2012;36(2):305–311.
19. Smith SM. Fast robust automated brain extraction. Hum Brain Mapp 2002;17(3):143–155.
20. Zhang Y, Brady M, Smith S. Segmentation of brain MR images through a hidden Markov random field model and the expectation-maximization algorithm. IEEE Trans Med Imaging 2001;20(1):45–57.
21. Smith SM, Jenkinson M, Woolrich MW, et al. Advances in functional and structural MR image analysis and implementation as FSL. Neuroimage 2004;23(Suppl 1):S208–S219.

22. Jenkinson M, Smith S. A global optimisation method for robust affine registration of brain images. Med Image Anal 2001;5(2):143–156.

23. Groenink M, de Roos A, Mulder BJ, Spaan JA, van der Wall EE. Changes in aortic distensibility and pulse wave velocity assessed with magnetic resonance imaging following beta-blocker therapy in the Marfan syndrome. Am J Cardiol 1998;82(2):203–208.

24. Leeson CP, Robinson M, Francis JM, et al. Cardiovascular magnetic resonance imaging for non-invasive assessment of vascular function: validation against ultrasound. J Cardiovasc Magn Reson 2006;8(2):381–387.

25. Dogui A, Redheuil A, Lefort M, et al. Measurement of aortic arch pulse wave velocity in cardiovascular MR: comparison of transit time estimators and description of a new approach. J Magn Reson Imaging 2011;33(6):1321–1329.

26. National Cholesterol Education Program (NCEP) Expert Panel on Detection, Evaluation, and Treatment of High Blood Cholesterol in Adults (Adult Treatment Panel III). Third Report of the National Cholesterol Education Program (NCEP) Expert Panel on Detection, Evaluation, and Treatment of High Blood Cholesterol in Adults (Adult Treatment Panel III) final report. Circulation 2002;106(25):3143–3421.

27. Drazner MH, Dries DL, Peshock RM, et al. Left ventricular hypertrophy is more prevalent in blacks than whites in the general population: the Dallas Heart Study. Hypertension 2005;46(1):124–129.

28. Fan J, Li R. Variable selection via nonconcave penalized likelihood and its oracle properties. J Am Stat Assoc 2001;96(456):1348–1360.

29. Laurent S, Katsahian S, Fassot C, et al. Aortic stiffness is an independent predictor of fatal stroke in essential hypertension. Stroke 2003;34(5):1203–1206.

30. Laurent S, Alivon M, Beaussier H, Boutouyrie P. Aortic stiffness as a tissue biomarker for predicting future cardiovascular events in asymptomatic hypertensive subjects. Ann Med 2012;44(Suppl 1):S93–S97.

31. Lim HE, Park CG, Shin SH, Ahn JC, Seo HS, Oh DJ. Aortic pulse wave velocity as an independent marker of coronary artery disease. Blood Press 2004;13(6):369–375.

32. Boutouyrie P, Tropeano AI, Asmar R, et al. Aortic stiffness is an independent predictor of primary coronary events in hypertensive patients: a longitudinal study. Hypertension 2002;39(1):10–15.

33. Poels MM, Zaccai K, Verwoert GC, et al. Arterial stiffness and cerebral small vessel disease: the Rotterdam Scan Study. Stroke 2012;43(10):2637–2642.

34. Brandts A, van Elderen SG, Westenberg JJ, et al. Association of aortic arch pulse wave velocity with left ventricular mass and lacunar brain infarcts in hypertensive patients: assessment with MR imaging. Radiology 2009;253(3):681–688.

35. van Elderen SG, Brandts A, van der Grond J, et al. Cerebral perfusion and aortic stiffness are independent predictors of white matter brain atrophy in type 1 diabetic patients assessed with magnetic resonance imaging. Diabetes Care 2011;34(2):459–463.

36. Schillaci G, Mannarino MR, Pucci G, et al. Age-specific relationship of aortic pulse wave velocity with left ventricular geometry and function in hypertension. Hypertension 2007;49(2):317–321.

37. Westerhof N, O'Rourke MF. Haemodynamic basis for the development of left ventricular failure in systolic hypertension and for its logical therapy. J Hypertens 1995;13(9):943–952.

38. Toprak A, Reddy J, Chen W, Srinivasan S, Berenson G. Relation of pulse pressure and arterial stiffness to concentric left ventricular hypertrophy in young men (from the Bogalusa Heart Study). Am J Cardiol 2009;103(7):978–984.

39. Mitchell GF. Arterial stiffness and wave reflection in hypertension: pathophysiologic and therapeutic implications. Curr Hypertens Rep 2004;6(6):436–441.

40. Girerd X, Laurent S, Pannier B, Asmar R, Safar M. Arterial distensibility and left ventricular hypertrophy in patients with sustained essential hypertension. Am Heart J 1991;122(4 Pt 2):1210–1214.

41. Liu ZR, Ting CT, Zhu SX, Yin FC. Aortic compliance in human hypertension. Hypertension 1989;14(2):129–136.